NONLINEAR DYNAMICS OF
SELF-SYNCHRONIZING SYSTEMS

by

M. de Sousa Vieira, A.J. Lichtenberg,
and M.A. Lieberman

NONLINEAR DYNAMICS OF
SELF-SYNCHRONIZING SYSTEMS

by

M. de Sousa Vieira, A.J. Lichtenberg,
and M.A. Lieberman

ELECTRONICS RESEARCH LABORATORY

College of Engineering
University of California, Berkeley
94720

NONLINEAR DYNAMICS OF
SELF-SYNCHRONIZING SYSTEMS

by

M. de Sousa Vieira, A.J. Lichtenberg,
and M.A. Lieberman

ELECTRONICS RESEARCH LABORATORY

NONLINEAR DYNAMICS OF SELF-SYNCHRONIZING SYSTEMS

M. de Sousa Vieira, A. J. Lichtenberg and M. A. Lieberman

Department of Electrical Engineering and Computer Sciences

and the Electronics Research Laboratory

University of California

Berkeley CA 94720

ABSTRACT

We investigate the self-synchronization of nonlinear systems. The particular system considered is two digital coupled phase locked loops. It is shown that the overall dynamics is far more complicated than that of a single loop, which is governed by a one-dimensional circle map. In the case of two coupled loops we observe that the dynamics is governed by explicit mapping equations only for certain regions of the parameter space. In the regions for which mapping equations can be derived we find the universality class of the coupled loop. Using such a two loop system as a transmitter of a chaotic signal, it is shown how a third loop can synchronize with this signal. Our results may have applications for the problem of secure communications.

I. INTRODUCTION

A synchronizing system is one that locks the phase of an output signal (the receiver) to an input signal (the transmitter). A particular device that accomplishes this is a phase locked loop (PLL). Such devices have proved useful in a variety of communication applications, including modulation and demodulation, and noise reduction[1]. PLL's can be either analog or digital (DPLL), both being easy to realize and obeying equations that are convenient to analyze[2]. In particular, the DPLL's have mapping representations that allow straightforward numerical investigation of their nonlinear properties, that is, dynamics far from the locked state[3,4,5,6].

In the usual synchronization system, the transmitter signal is a single carrier frequency that corresponds to a sinusoidal signal at constant amplitude and phase, and a phase locked loop in the receiver is used to lock the receiver phase to that of the transmitter. Recently, it has been shown[7] that a dynamical system of three differential equations, exhibiting chaos, can be used to transmit a signal to a subsystem of those equations, in such a manner that the subsystem is synchronized with the primary chaotic system. This opens up an interesting new possibility that the phase of a receiver can be locked to that of a transmitter even if the transmitted signal is chaotic, i.e., consisting of a continuous spectrum of carrier frequencies. Such synchronized systems can have applications to problems of secure communications and may be an alternative to conventional spread spectrum systems.

A particularly simple DPLL is a first-order nonuniformly sampling loop, which, as we shall discuss in Section II, has a circle map representation. If we couple two such DPLL's together, the resulting dynamics can be far more complicated than that of a single loop, because the loops can switch asynchronously, so that far from the locked state one DPLL may change state more than once while the other is not changing state. Thus unlike the usual coupled map lattices[8], there is no explicit mapping representation for such coupled devices.

In the following sections we describe the behavior of a coupled system consisting of two first order DPLL's in which the output of the second loop serves as the input for the

first loop, and vice-versa. We call such a system self-synchronizing. For some regions of the parameter space the usual properties associated with a single circle map persist, while for other parameters the overall dynamics is more complicated. We then show how two self-synchronized first-order DPLL's can be used to implement a transmitting system, that generates a chaotic carrier signal, and how a third loop can be used as a receiving system, that locks to the phase of the chaotic carrier.

In section II we derive the dynamics of a single loop, showing that the dynamics can be described by a simple one-dimensional circle map. Such maps are known to have a rich dynamical behavior[9], including quasiperiodic motion, regions of phase-locking, period-doubling to chaos and intermittency. Coupling two such DPLL's together such that the output of each loop is the input for the other loop, we obtain the algorithm for iterating the coupled system and obtain explicit mapping equations valid for some regimes. In section III we analyze the dynamics of the two-coupled-loop system in detail and obtain numerically the conditions for the self-synchronized chaotic motion. In Section IV we introduce the receiving element and demonstrate phase locking of the receiver to the chaotic transmitted signal. We also study the effect of variation of the receiving loop parameters on the phase locking. The embodiment here has a particular simplicity that makes the concept both transparent and potentially useful. In Section V we summarize our results and describe some extensions to the concept.

II. SYSTEM DESCRIPTION

A. Single Loop

A block diagram of a single, first-order, nonuniformly sampling DPLL is shown in Fig. 1. It consists of a sample-and-hold (SH) and a variable frequency oscillator (VFO). During the operation, the SH takes a discrete sample $s(t_k)$ of the incoming signal at a sampling time t_k, when the VFO signals it to do so at a positive going zero crossing. The sample is used to control the frequency of the VFO according to a given function $\omega(s)$ in such a way as to decrease the phase difference between the incoming signal and the oscillator output. As a result, there is a possibility of locked behavior when the oscillator frequency adjusts

itself to the input frequency and locks to its phase, hence sampling always at the same point on the input signal.

Consider the case in which the incoming signal is given by $s(t) = A\sin(\omega t + \theta_0)$. Suppose that the period of the oscillator is linearly related to $s(t_k)$ as

$$T_{k+1} = T_0 - bs(t_k),\tag{1}$$

where $T_0 = 2\pi/\omega_0$. The center frequency ω_0 is the frequency of the VFO in the absence of the applied signal. It was shown by Gil and Gupta[3] that in a loop governed by Eq. (1) the evolution of the phase difference between signal and oscillator output is described by a nonlinear difference equation given by

$$\phi(t_{k+1}) = \phi(t_k) - \omega bA \sin\phi(t_k) + 2\pi\omega/\omega_0.\tag{2}$$

Equation (2) is the well known sine-circle map, which has been studied in detail as a prototype that presents the quasi-periodic route to chaos[9]. In the context of DPLL's, Eq. (2) was studied by several authors[4], after Gil and Gupta.

In the usual practical devices, where the frequency, not the period, is linearly related to the input sample as

$$\omega(t_{k+1}) = \omega_0 + bs(t_k),\tag{3}$$

then another map is obtained for the phase difference:

$$\phi(t_{k+1}) = \phi(t_k) + \frac{2\pi\omega}{\omega_0 + bA\sin\phi(t_k)}.\tag{4}$$

This is also of the form of a circle map, and displays the usual behavior associated with such maps[5].

B. Coupled Self-Synchronizing Loops

The self-synchronization system of two coupled DPLL's, for which the forcing input in one loop is the oscillator output of the other loop is shown in Fig. 2. We study here only the case in which the frequency of the oscillator is linearly related to the input sample according to Eq. (3). Preliminary calculations show that if the coupled system is governed by Eq. (1) similar qualitative results are obtained.

4

In Fig. 3 we show a diagram that exemplifies the dynamics of the coupled system. The signals in the figure, which are taken to be sinusoidal, represent the time varying output of the VFO's. Each time that one of these signals cross the zero axis in the positive derivative sense, then the oscillator sends a signal to the SH and an input sample is taken from the VFO output of the other loop. The loop that samples switches its frequency to a new value according to Eq. (3). The evolution of the system follows the steps described by the following algorithm:

Given the frequencies ω_1, ω_2 and the phases θ_1, θ_2 of the two VFO's at $t = 0$ then:

0) Initialization: Find what should have been the last sampling time t_i and the next sampling time t'_i for both loops ($i = 1, 2$)

$$t_i = \frac{-\theta_i}{\omega_i}, \tag{5a}$$

$$t'_i = \frac{2\pi - \theta_i}{\omega_i}. \tag{5a}$$

1) Search over the two DPLL's to find the loop l with the smallest time for the next sampling; that is, find l such that

$$t'_l = \text{smaller}(t'_i), \qquad (i = 1, 2). \tag{6}$$

2) Calculate the input sample value, which is taken from the output signal of the other VFO:

$$s_i(t'_l) = A \sin \phi_i, \qquad (i \neq l) \tag{7}$$

where

$$\phi_i = \omega_i(t'_l - t_i). \tag{8}$$

3) Update the frequency of the loop l according to Eq. (3)

$$\omega'_l = \omega_0 + b_l s_i(t'_l). \tag{9}$$

4) Set $t_l = t'_l$ and $t'_l = t_l + 2\pi/\omega'_l$. Go to step 1.

For any time t, the system state is determined by four variables, that is, the frequencies and the phases of the two loops. However, observe that the system state changes only at

the sampling instants, $\phi_1 = 0 \pmod{2\pi}$ or $\phi_2 = 0 \pmod{2\pi}$. At these instants we need to know only the two variables (ω and ϕ) of the loop that does not sample, because $\phi = 0$ and $\omega = \omega_0 + bs(t_k)$ for the loop that samples. In this way, we can evolve the system at discrete times in a reduced variable space. For a surface of section, say $\phi_2 = 0$, because $\omega_2 = \omega_2(\omega_1, \phi_1)$, the dynamics can be visualized in a two dimensional subspace (ω_1, ϕ_1). The evolution is therefore determined by three variables, (say $\phi_2(\equiv 0)$, ω_1 and ϕ_1), rather than the four variables of the total phase space. We note that we do not have an explicit mapping, as in the case of a single loop. The system evolution is described by the algorithm given above. We find that two equations for the phases govern the dynamics of the coupled system, namely

$$\phi_i' = \phi_i + 2\pi \left(\frac{\omega_0 + b_i \sin \phi_j}{\omega_0 + b_j \sin \phi_i} \right), \tag{10a}$$

and

$$\phi_i' = (2\pi - \phi_j) \left(\frac{\omega_0 + b_i \sin \phi_j}{\omega_0 + b_j \sin \phi_i} \right), \tag{10b}$$

where i, j refers to the index of the loop, 1 or 2. The phases that appear on the right hand side of Eqs. (10) are the phases associated with the last sampling times of loops i and j, and the primes refer to the next sampling time. The first equation applies when one loop samples at two or more consecutive times while the other loop does not sample. The second equation applies when successive sampling times originate from alternate loops. Note that we have taken $A = 1$, since it appears always multiplied by the gain b, and we can take this product as a unique parameter. Also, we consider that the b's are in principle distinct for the two loops, whereas the center frequencies ω_0's are the same for both. This is done to reduce the dimensionality of the parameter space.

When we evolve the dynamics, we do not know in principle the sequence in which Eqs. (10) will be applied; this will depend on the loop parameters. In a general situation we have to follow the steps of the algorithm described previously.

III. RESULTS

Following the above dynamics we explore numerically the two coupled DPLL system by varying the external parameters ω_0 and b's, and a complex behavior is observed. Initially

we consider two identical loops, i.e., the parameters are both the same. In this situation we expect that we will not lose any important aspect of the dynamical evolution by observing the dynamics of one of the loops. We therefore study the evolution of one loop at the sampling times of the other, that is, we study the system at the the surface of section $\phi_i = 0$, where i is chosen to be 1 or 2. Without loss of generality we can take $\omega_0 = 1$.

In Fig. 4(a) we show the bifurcation diagram for ϕ_1 at $\phi_2 = 0$ as a function of $b \equiv b_1 = b_2$ for $\omega_0 = 1$, after the transient period has died out. The dynamics is characterized by periodic cycles and a chaotic regime, which is interwoven with periodic windows, as in many dissipative dynamical systems. Initially the system locks in a period one cycle. Then it bifurcates to a period two cycle where a 'splitting' bifurcation appears[10]. A splitting bifurcation is observed when multiple basins of attraction emerge; the initial condition determines which basin of attraction will be chosen by the system. The new stable attractors have the same periodicity as the attractors which become unstable. This phenomenon has interesting consequences for the synchronization of coupled DPLL's, as we shall see in section IV. Following the splitting bifurcation we observe a cascade of period doubling bifurcations and beyond this a chaotic regime. By varying the center frequency ω_0, we observed a similar qualitative behavior, in a reverse order. This is easily understood in terms of the trajectory of passing through an Arnold tongue (region of phase locking) in the parameter space. For $b_1 \neq b_2$ we observe period doubling sequences in the parameter plane, and also more complicated bifurcation diagrams for certain choices of the parameters, such as the one shown in Fig. 4(b).

The phase diagram in the (b_1, b_2) plane for $\omega_0 = 1$ is shown in Fig. 5. The black regions represent the parts of the parameter space with a very large period, which we use as an approximate test that the system is chaotic at those points. As expected, the region of stability is mostly concentrated about the lower values of the parameter b. For higher values of b there is stochastic behavior mixed with some tongues of stability.

As stated previously, we do not know in principle the sequence in which Eqs. (10) will be applied. However we observe numerically that anywhere within the period doubling sequence, at the periodic orbit, the loops sample in a fixed time sequence, such that one loop samples twice, then the other loop also samples twice, then the first one repeats the

7

process, following exactly the sequence shown in Fig. 3. We observed this for several choices of the initial conditions and parameter values. We believe that this is a generic process in the bifurcation cascade.

For the parameter values for which the dynamics lies within the bifurcation sequence we can write mapping equations to describe the evolution of the system. They are given by

$$\phi_1' = \phi_1 + 2\pi \left(\frac{\omega_0 + b_1 \sin \phi_2}{\omega_0 + b_2 \sin \phi_1} \right), \tag{11a}$$

$$\phi_2' = (2\pi - \phi_1') \left(\frac{\omega_0 + b_2 \sin \phi_1'}{\omega_0 + b_1 \sin \phi_2} \right), \tag{11b}$$

$$\phi_2'' = \phi_2' + 2\pi \left(\frac{\omega_0 + b_2 \sin \phi_1'}{\omega_0 + b_1 \sin \phi_2'} \right), \tag{11c}$$

$$\phi_1'' = (2\pi - \phi_2'') \left(\frac{\omega_0 + b_1 \sin \phi_2''}{\omega_0 + b_2 \sin \phi_1'} \right). \tag{11d}$$

From the above equations, one can calculate the jacobian matrix for the transformation $\phi_i \rightarrow \phi_i''$. Initially we calculate the matrix that transforms $\phi_i \rightarrow \phi_i'$, and then multiply this matrix by the one that transforms $\phi_i' \rightarrow \phi_i''$. The trace of the resulting jacobian matrix gives a measure of the stability of the orbit. The most stable orbits have null trace, giving the parameter value that corresponds to the optimum stable system performance for a given cycle. We show in Table 1 the values of the parameter $b \equiv b_1 = b_2$ at these superstable orbits of the bifurcation cascade, for $\omega_0 = 1$. Because of the splitting bifurcation, two superstable values are found for the 2-cycle. The sequence of b's converges with a geometric ratio given by $\delta \approx 4.6692...$, as in quadratic mappings. Thus the two coupled DPLL's, when described by Eqs. (11), have the same universality class as dissipative systems governed by a quadratic map. At the period doubling bifurcations the trace of the jacobian matrix is -1, as expected; for the splitting bifurcation it is 1.

The border of stability of the period one cycle can be obtained analytically by explicit examination of the Jacobian matrix near $\phi_1 = \phi_2 = 0$ which is the stable sampling phase of the 1-cycle. Suppose that one perturbs the frequency of one loop in such a way that its

frequency changes to $\omega_0 + \epsilon$; then one finds that at the next sampling time, the perturbation in the frequency with respect to the locked state will be

$$\epsilon' = \epsilon \left[1 - \frac{2\pi}{\omega_0}(b_1 + b_2) \right].$$

(12)

with the bracketed term being the trace of the Jacobian matrix. At the superstable cycle the perturbation vanishes, and therefore

$$b_1 + b_2 = \frac{\omega_0}{2\pi}.$$

(13)

The period doubling bifurcation will occur when ϵ'/ϵ is -1. Thus, at this point

$$b_1 + b_2 = \frac{\omega_0}{\pi}.$$

(14)

We studied the chaotic regime in the phase vs. frequency plot, by taking a surface of section in which the phase of one (any one) loop is zero, as described previously. The point $b_1 = 0.15$, $b_2 = 0.55$ and $\omega_0 = 1$ has positive Liapunov exponent (we used the algorithm of Ref. [11] in the calculation of the exponent). We have chosen these parameters to plot in Fig. 6 the phase vs. frequency of loop 1 at $\phi_2 = 0$. A magnification of that figure shows a finely structured group of neighboring trajectories, which is a characteristic of strange attractors. Observe that for $\phi_1 \to 0$ the only possible value for ω_1 is $\omega_1 \approx \omega_0$. This is easily understood when we follow the dynamics shown in Fig. 3. Every time that the phase of loop 1 is near 2π, then the input sample taken by loop 2 will be near zero. Consequently the frequency of loop 2 will be close to ω_0. The next loop to sample will be loop 1, and for an analogous reason its frequency will also be close to the center frequency.

IV. SYNCHRONIZATION TO A CHAOTIC SIGNAL

We consider in this section the synchronization to a chaotic signal produced by the coupled DPLL's. The idea of synchronizing to chaotic signals was introduced recently by Pecora and Carroll[7]. They have shown that certain subsystems of nonlinear, chaotic systems can be made to synchronize by linking them with common signals. The synchronization is obtained from the influence of the chaotic driving system (the transmitter) on

9

the response system (the receiver) while the driving system remain unperturbed. In their work, Pecora and Carroll investigated low-dimensional systems described by ODE's. They showed numerically that the necessary condition for the subsystem to follow the master system is that it have only negative Liapunov exponents. The concept of synchronized chaos was applied recently to spatially extended systems, consisting of an array of coupled lasers[11]. It was shown that there are extended systems where the synchronized chaos corresponds to spatial order and temporal disorder. By varying the external parameters this scenario breaks down and spatiotemporal chaos, or turbulence, may appear.

The system we studied is shown in Fig. 7. The driving (or master) system is the two coupled DPLL system studied in the previous sections. The signal that originates from one of the VFO's (in this case the second one) is used to feed a slave system which consists of one single DPLL (the third loop). For the system shown, we investigated the parameter values that yield synchronization of the signals originated from loop 1 and loop 3. We observe that there is a range of the parameter space where the slave system completely synchronizes to the driving system, whereas in other regions they seem practically uncorrelated. We showed in Fig. 5 the region of the parameter space where chaotic behavior is expected for the driving system. If we pick the point $b_1 = 0.15$ and $b_2 = 0.55$, for which we verified that the temporal dynamics is chaotic, we observe that at this point, for $b_3 = b_1$, the temporal evolution of the outputs of VFO 1 and VFO 3, after a transient period, are completely identical. This is illustrated in Fig. 8, where we plot ϕ_3 against ϕ_1, for the surface of section $\phi_2 = 0$. Thus, as in the case of coupled lasers[11] we observe a regime of temporal chaos and spatial order. The result here might have been expected, because, as we can see from Fig. 5, b_1 and b_3 are chosen such that loops 1 and 3 are operating in a regime that would be phase locked to an appropriate sinusoidal input signal. With a chaotic input, we cannot expect a phase locked output, but it is intuitive to expect that the stable loops will have identical outputs for identical inputs, as observed.

Those expectations are verified globally in Fig. 9, in which the white region indicates the parameter space of synchronization. The necessary condition for the existence of synchronized chaos is that all the Liapunov exponents of the subsystem must be negative, as shown by Pecora and Carroll. We observe that the value $b_1 = b_3 \leq 0.35$ roughly

marks the border of synchronization. This corresponds approximately to the region of the parameter space, as seen in Fig. 5, of regular motion for loop 1 and loop 3. Thus, even if loop 2 is chaotic, i.e., $b_2 \gtrsim 0.35$, synchronization may be achieved between loop 1 and loop 3.

When $b_1 = b_3 \gtrsim 0.35$, (the cross-hatched portion) synchronization of loop 1 and loop 3 is not observed in most part of the parameter space. This is consistent with their chaotic response to any input signal for these parameters. For this regime the resulting chaotic attractor appears to lie in in a higher dimensional space, as is shown in Fig. 10 . Contrast this figure with Fig. 6, which shows a chaotic attractor in the region of synchronization. Theoretical questions remain concerning such problems as quantitative differences between different types of attractor, characterizing them by fractal dimension, etc.

For parameter values where multiple basins of attraction are found, the synchronization may not occur. One clear example in the figure is the region of the splitting bifurcations ($b_1 \approx b_2 \approx 0.33$). There we have two separate 2-cycles, such that the system does not synchronize, if loops 1 and 3 settle in different basins of attraction.

In a practical situation, it would not be possible to make b_1 and b_3 identical. Pecora and Carroll addressed this question for systems of differential equations and found that the synchronization persists, but with some error between the dynamical values of the master and slave system. We expect this same behavior in our coupled loop transmitter-receiver system, which, indeed, turns out to be the case. In Fig. 11 we make $b_3 = 0.1$ and use the same values $b_1 = 0.15$ and $b_2 = 0.55$ given in Fig. 8. We observe that in this case, when loop 3 is not completely identical to loop 1, the synchronization is degraded, but the loops have retained much of their correlation.

V. CONCLUSIONS AND DISCUSSIONS

We have seen that a self-synchronizing system of two coupled DPLL's has parameter ranges in which its behavior is one to one with its simpler relative, a single synchronizing DPLL. The larger phase space allows more complicated behavior over other parameter ranges, and some of the similarities and differences are noted in our study. In particular the

11

sequence of bifurcations, leading to chaos, can be more complicated than period doubling, as seen in Fig. 4(b). The chaos, itself, looks different when observed on the output of the two loops, in the case where the b's for both loops are chosen such that they are unstable, as seen in Fig. 10, when compared to the output of the loops if one of them is stable and the other unstable, as shown in Fig. 6.

One key property of a self-synchronizing system of practical interest is that it can transmit a signal in the chaotic state that can be synchronized in time with a receiver. This synchronization to chaos, demonstrated in Fig. 8, opens up new possibilities for communications systems. An exploration of the parameter range over which synchronization can be achieved, shown in Fig. 9, indicates general agreement with the intuitive notion that the identical subsystems of the transmitter and receiver must be, themselves, stable. If the subsystem parameters are not identical, then the synchronization is not perfect, as shown in Fig. 11. However, information can still be transmitted.

It is clear that our study represents only a beginning of a detailed exploration of both the nonlinear dynamics and the communications possibilities. Some practical questions concern methods of modulation and implementation. Quantification of the degradation of synchronization, shown qualitatively in Fig. 11, is also important for practical applications.

A more general extension of this study concerns larger systems. It is clear from the above analysis that a repeater chain is more closely allied to the self-synchronizing system studied here than to a coupled map lattice, with one way coupling, that it might superficially resemble. If the repeater is put on a circle, then it is also self-synchronizing. Studies of more complex interconnections also suggest themselves.

REFERENCES

1. R. E. Best, *Phase Locked Loops* (McGraw-Hill Books Company, 1984).

2. W. C. Lindsey and C. M. Chie, *Proc. IEEE* **69**, 410 (1981).

3. S. Gil and S. C. Gupta, *IEEE Trans. Commun.* **20**, 454 (1972); *IEEE Trans. Aerosp. Electron. Syst.* **8**, 615 (1972).

4. A. Weinberg and B. Liu, *IEEE Trans. Commun.* **22**, 123(1974); N. A. D'Andrea and F. Russo, *IEEE Trans. Commun.* **26**, 11355 (1978); H. C. Osbourne, *IEEE Trans. Commun.* **28**, 1343 (1980).

5. G. M. Bernstein and M. A. Lieberman, *IEEE Trans. Circuits Systems* **37**,1157 (1990).

6. G. M. Bernstein, M. A. Lieberman and A. J. Lichtenberg, *IEEE Trans. Commun.* **37**, 1062 (1989).

7. L. M. Pecora and T. L. Carroll, *Phys. Rev. Lett.* **64**, 821 (1990).

8. J. P. Crutchfield and K. Kaneko, in *Directions in Chaos*, edited by Hao Bai-lin (World Scientific Publishing Co., Singapore (1987)).

9. S. J. Shenker, *Physica* (Utrecht) **5D**, 405 (1982); M. J. Feigenbaum, L. P. Kadanoff, and S. J. Shenker, *Physica* (Utrecht) **5D**, 370 (1982); D. Rand, S. Ostlund, J. Sethna, and E. Siggia, *Physica* (Utrecht) **6D**, 303 (1982).

10. J. Testa and G. A. Held, *Phys. Rev. A* **28**, 3085 (1983).

11. A. Wolf, J. B. Swift, H. L. Swinney and J. A. Vastano, *Physica* (Utrecht) **16D**, 285 (1985).

12. H. G. Winful and L. Rahman, *Phys. Rev. Lett.* **65**, 1575 (1990).

TABLE 1

Period	b
1	$\omega_0/2\pi$
2	0.2808560407
2	0.3496205907
4	0.3672296277
8	0.3715083345
16	0.3724198720
32	0.3726153586
64	0.3726572262

Table 1. Values of b for the superstable orbits, with $\omega_0 = 1$.
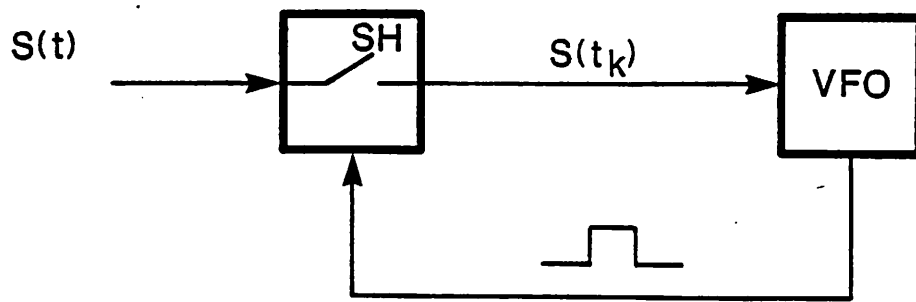
Fig. 1. Schematic representation of a single DPLL.
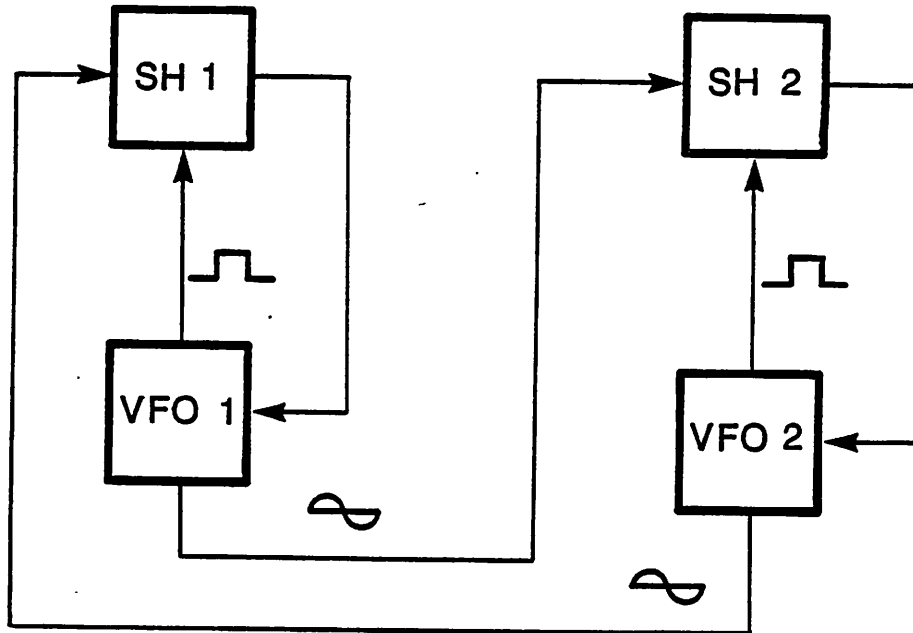
Fig. 2. Two coupled self-synchronizing DPLL's.
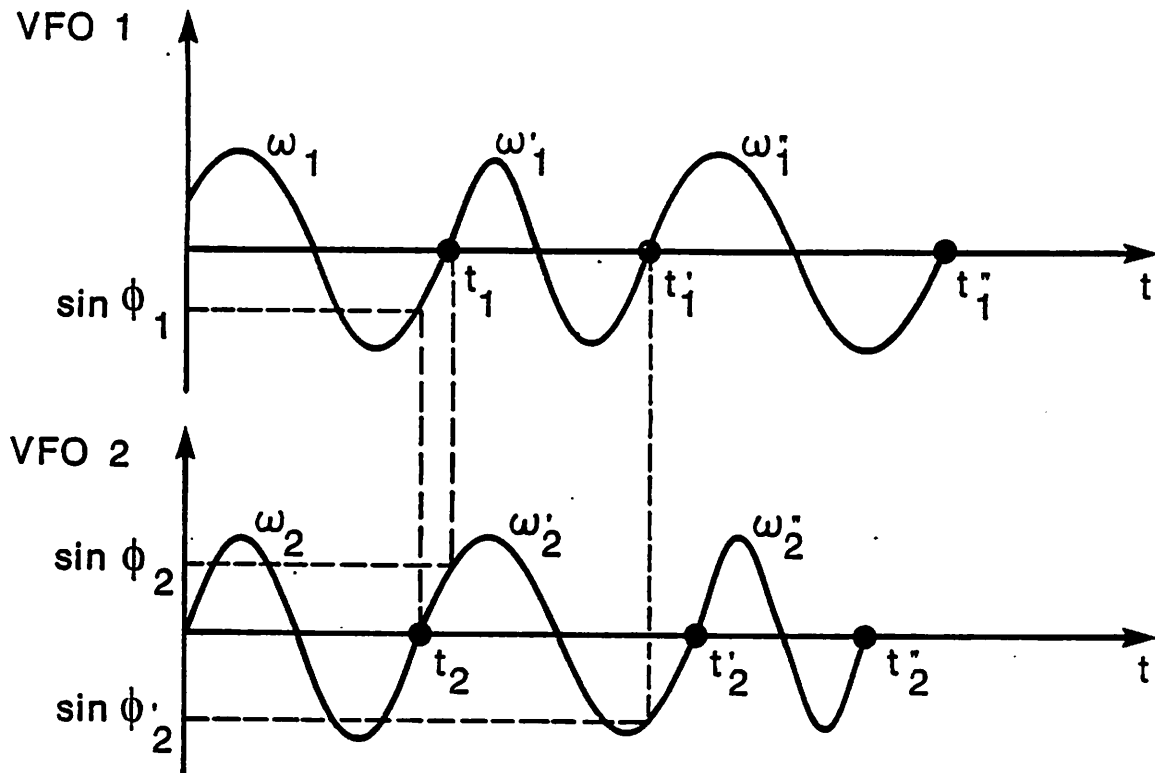
Fig. 3. Schematic representation of the dynamics of the two coupled DPLL's.
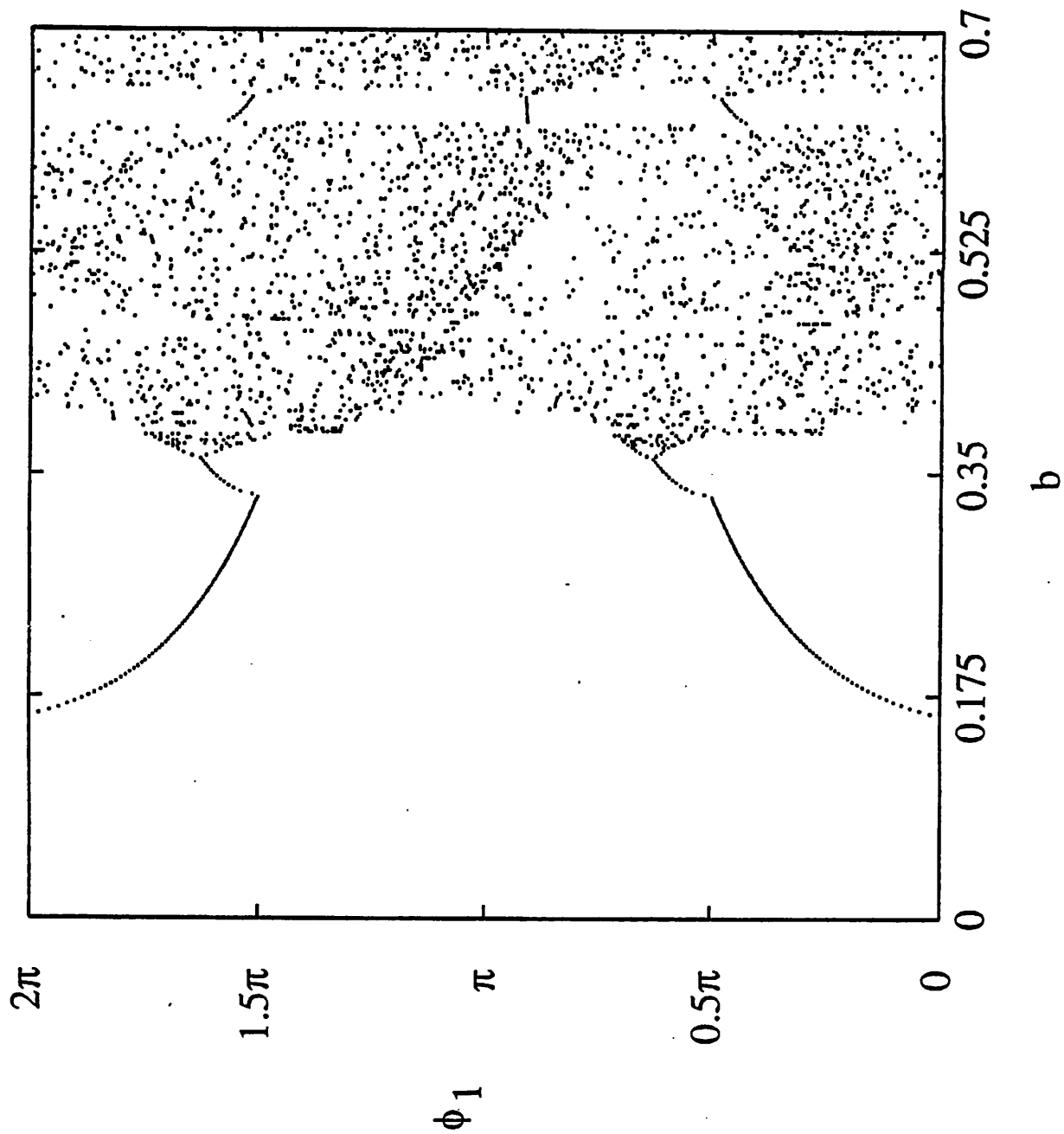
Figure 4a

Fig. 4. Bifurcation diagram for the phase of loop 1 at $\phi_2 = 0$ as a function of (a) $b \equiv b_1 = b_2$ and (b) b_1 for $b_2 = 0.35$, for $\omega_0 = 1$.
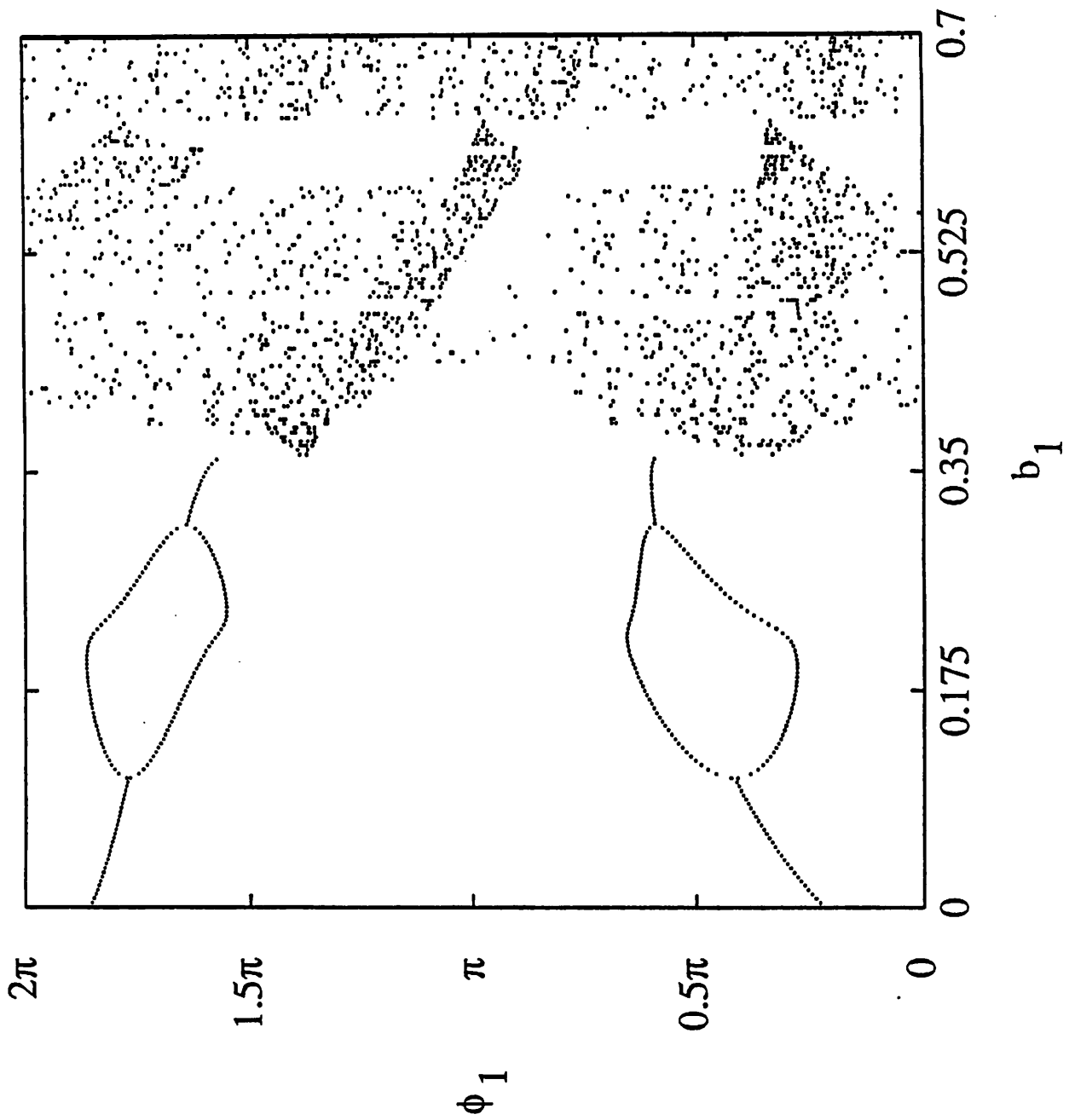
Figure 4b
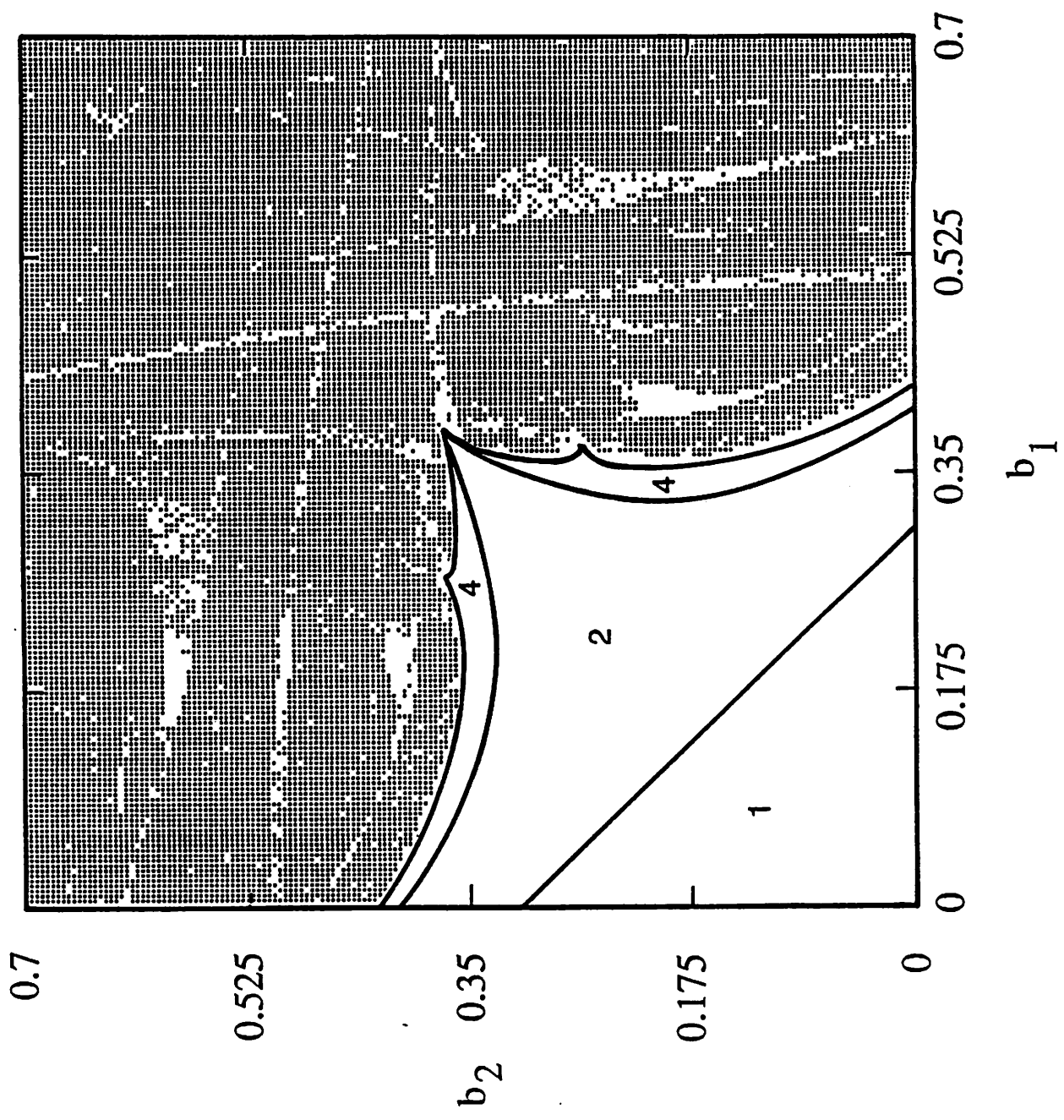
Fig. 5. Phase diagram b_1 versus b_2 for $\omega_0 = 1$, showing periodic orbits (labeled with the period) and chaotic regions (dotted).
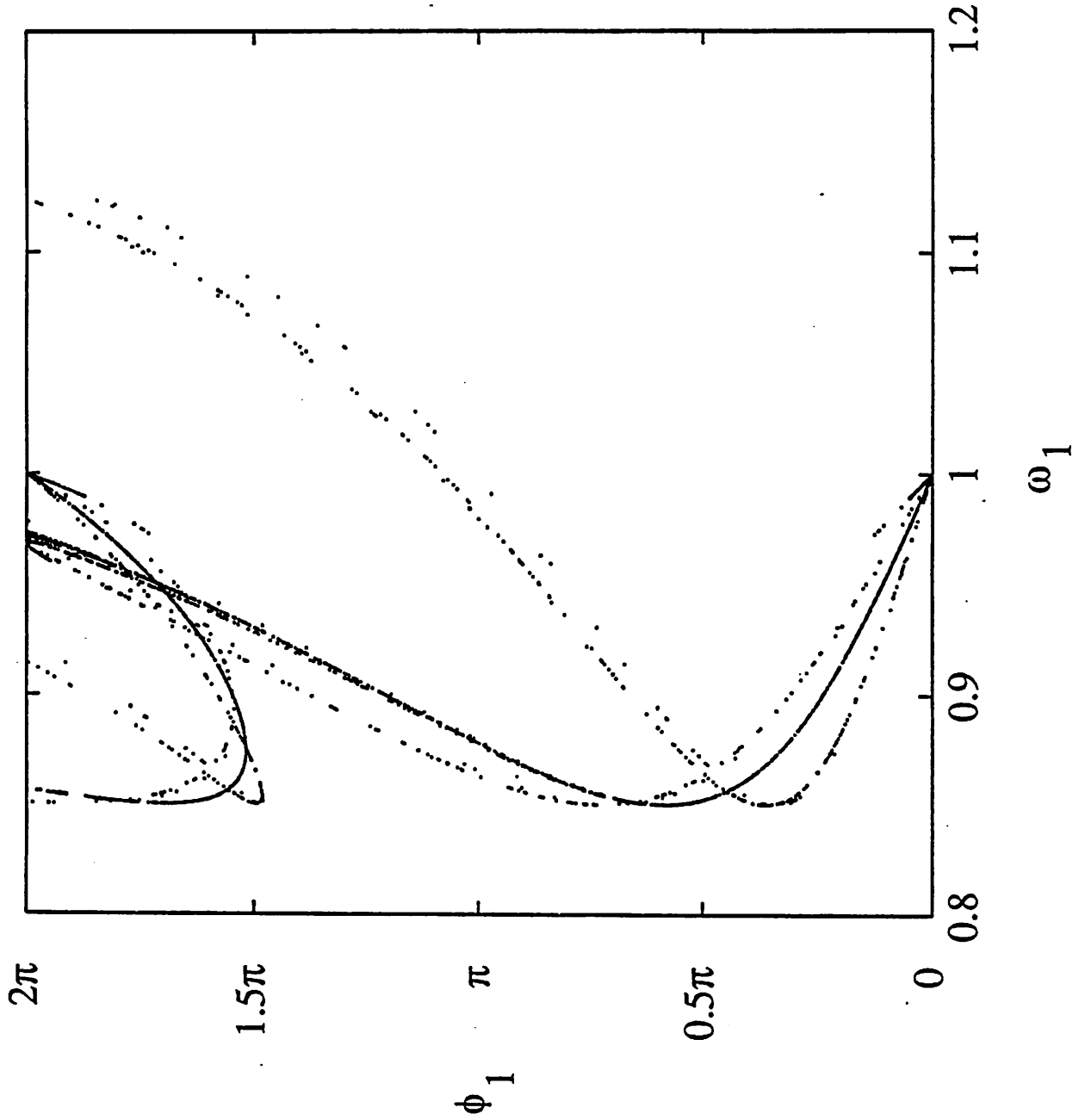
Fig. 6. Chaotic (or strange) attractor associated with loop 1 for $b_1 = 0.15$, $b_2 = 0.55$ and $\omega_0 = 1$ at $\phi_2 = 0$.
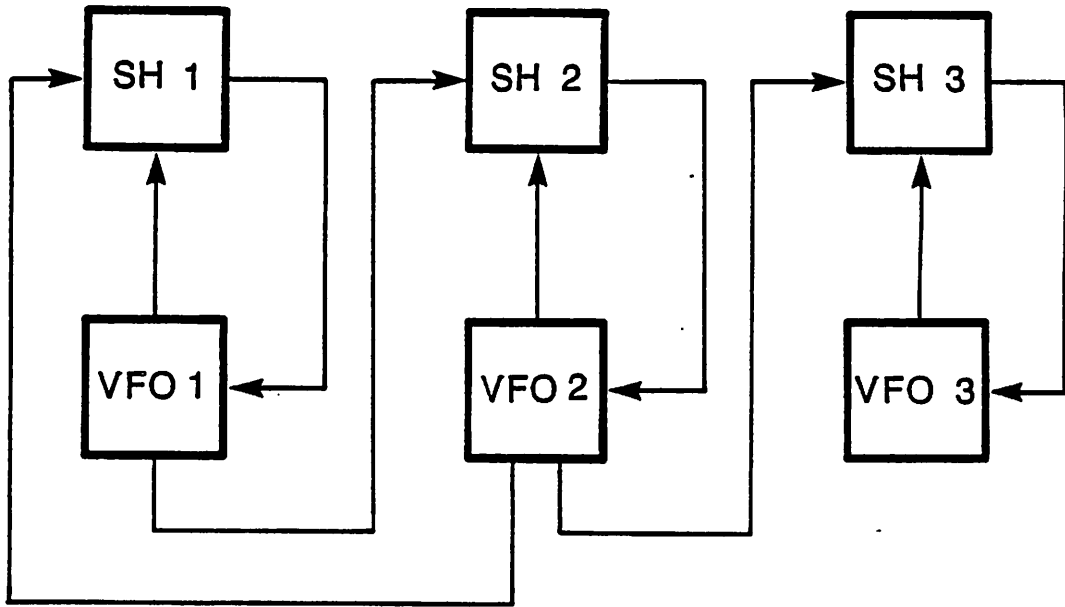
Fig. 7. Communication system consisting of three coupled DPLL's.
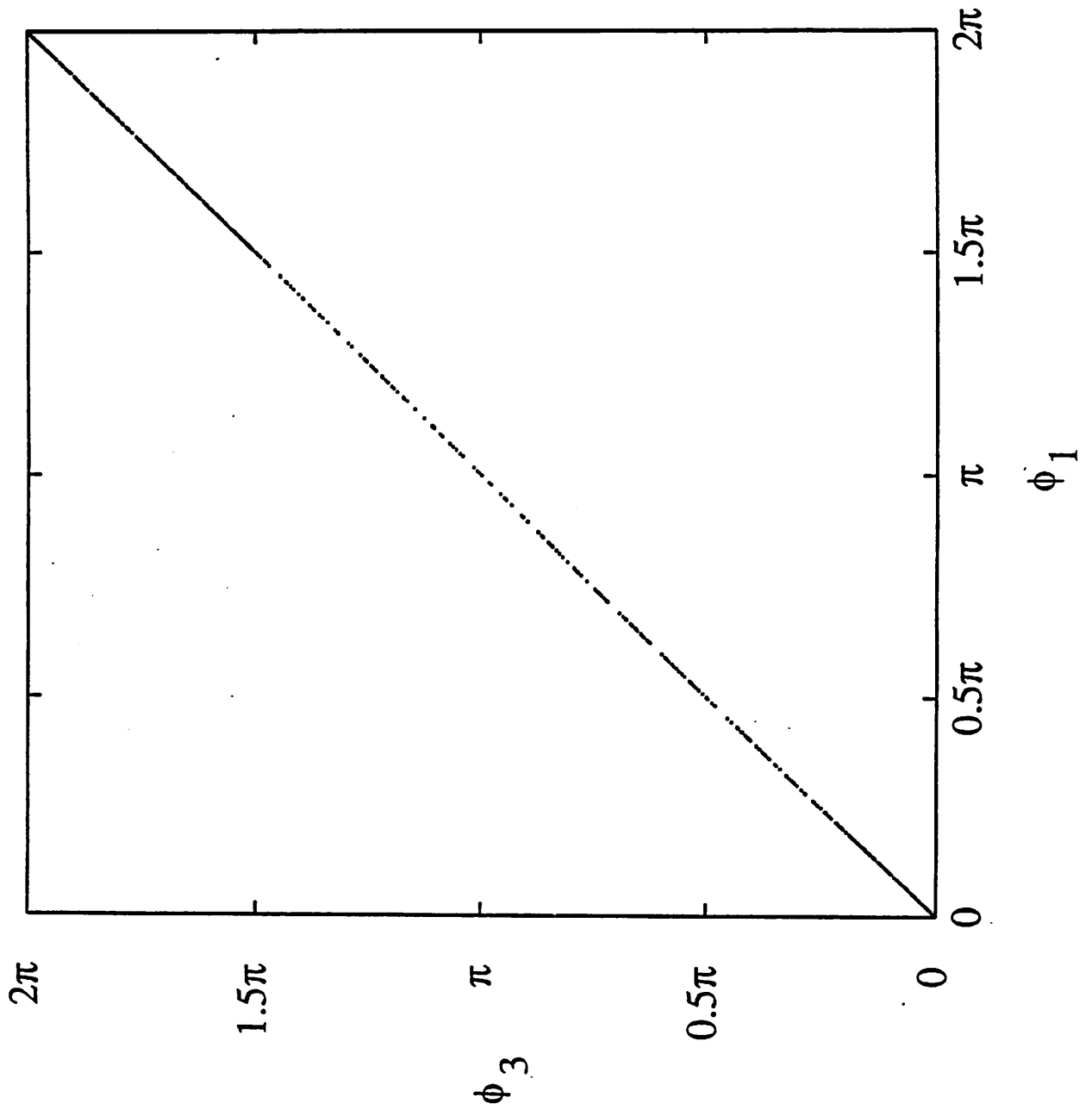
Fig. 8. ϕ_1 vs. ϕ_3 for $\omega_0 = 1$, $b_1 = b_3 = 0.15$ and $b_2 = 0.55$ at $\phi_2 = 0$.
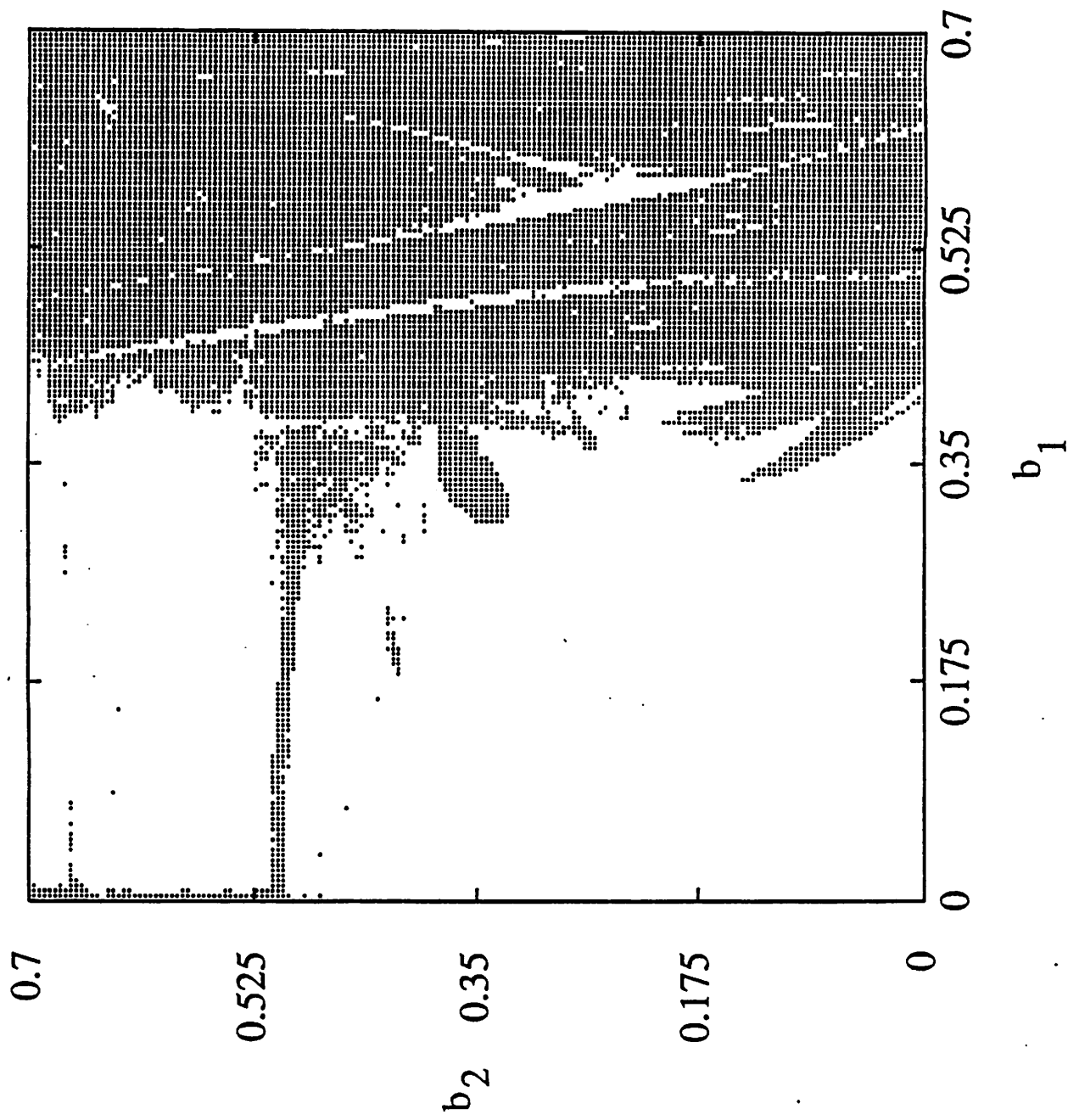
Fig. 9. Diagram showing the region of synchronization (white region) for three DPLL's.
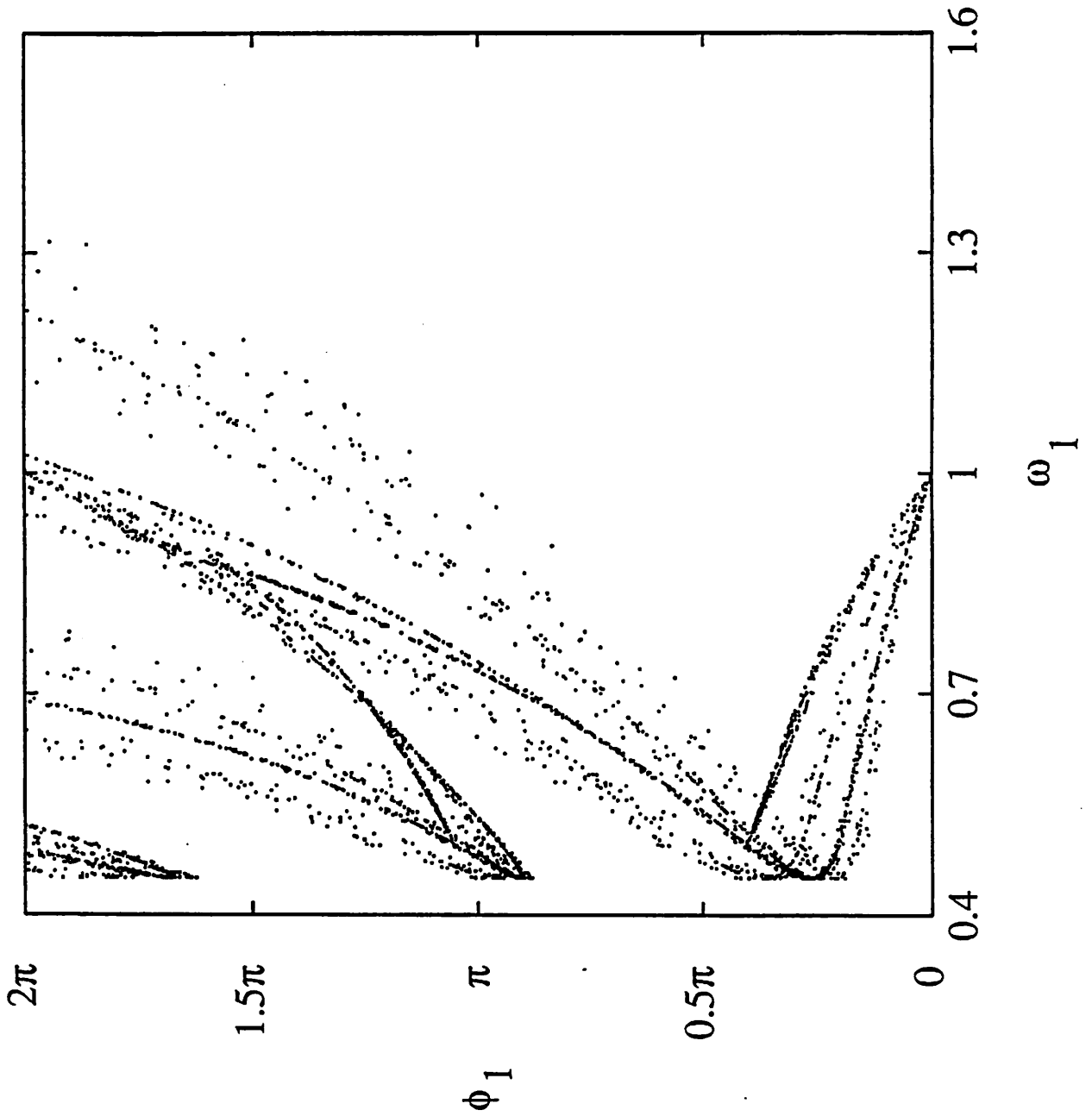
Fig. 10. Chaotic attractor associated with loop 1 (or loop 3) for $b_1 = b_2 = b_3 = 0.55$ and $\omega_0 = 1$ at $\phi_2 = 0$.
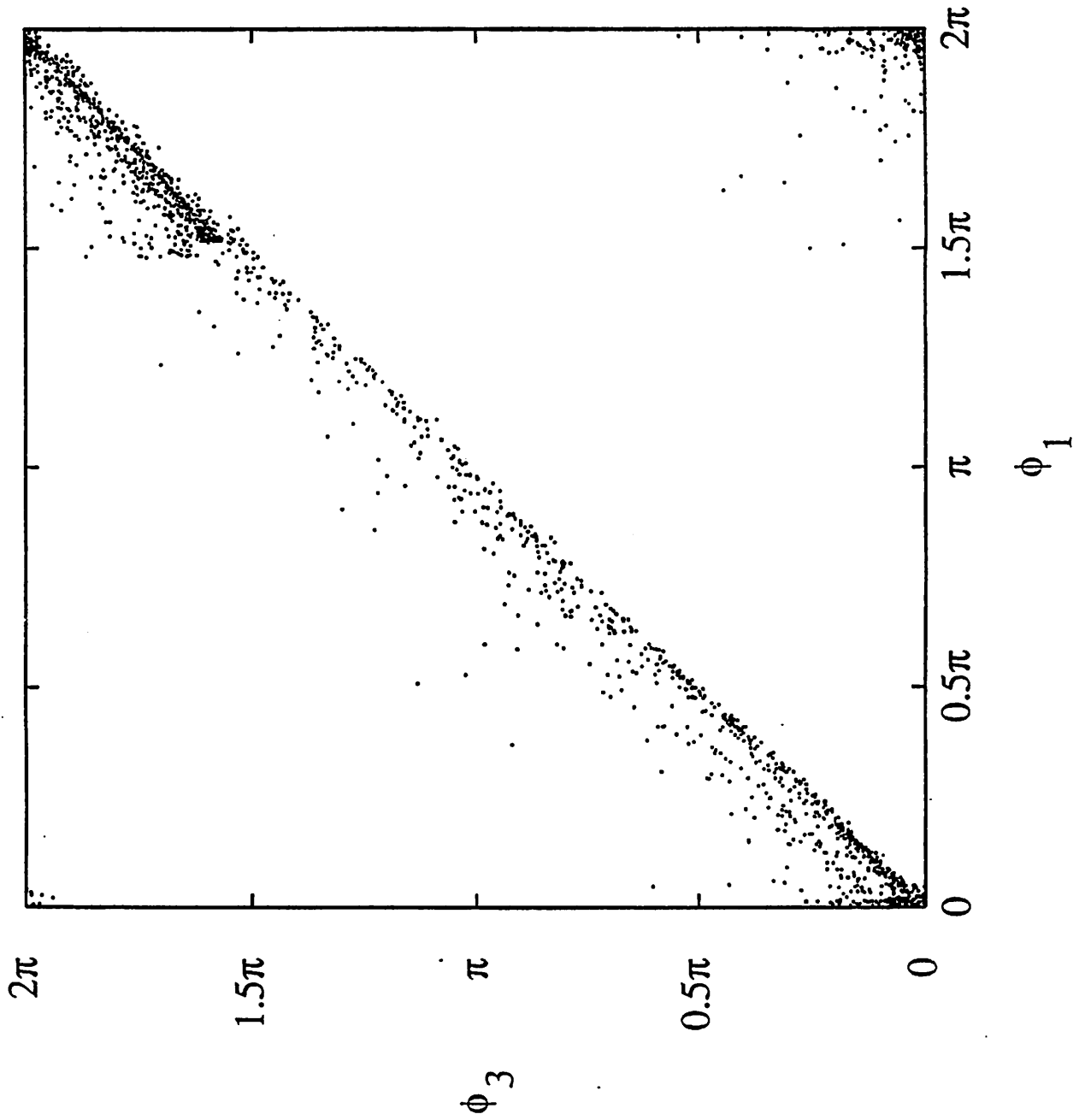
Fig. 11. ϕ_1 vs. ϕ_3 for $\omega_0 = 1$ and $b_1 = 0.15$, $b_2 = 0.55$, $b_3 = 0.1$ at $\phi_2 = 0$.